Electronic Supplementary Material (ESI) for Materials Advances.
This journal is © The Royal Society of Chemistry 2021

Electronic Supplementary Information: Fast Non-ambipolar Diffusion of Charge Carriers and the Impact of Traps and Hot Carriers on it in CSMAFA Perovskite and GaAs

Hannu P. Pasanen,*,† Maning Liu,† Hermann Kahle,‡ Paola Vivo,† and Nikolai V. Tkachenko*,†

†*Chemistry and Advanced Materials Group, Faculty of Engineering and Natural Sciences, Tampere University, Korkeakoulunkatu 8, FI-33720 Tampere, Finland*

‡*Optoelectronics Research Centre (ORC), Physics Unit / Photonics, Faculty of Engineering and Natural Sciences, Tampere University, Korkeakoulunkatu 3, FI-33720 Tampere, Finland*

E-mail: hannu.pasanen@tuni.fi; nikolai.tkachenko@tuni.fi

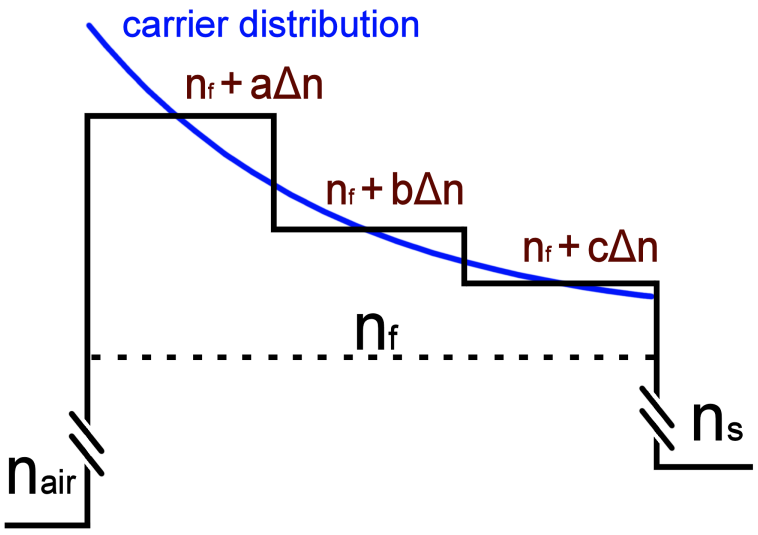

Figure S1: An example of the transient reflectance model and interference originating from the carrier distribution, where the solid black line is the refractive index across the model, the dashed line is the refractive index of the film before excitation and the blue line is the carrier distribution after excitation. A non-uniform carrier distribution causes a gradual change in the refractive index inside the film, which can be modelled by splitting the film into multiple layers, each with Δn multiplied by the average carrier concentration in that layer ($a > b > c$). These differences in the refractive index across the film cause interference in the transient reflectance signal, even if the film has high enough absorption to prevent interference from the film-substrate interface.

Transient reflectance model

Our thin-film interference (TFI) based transient reflectance model was originally introduced in our previous publications alongside the Matlab codes we used,[1,2] but we have since updated the Matlab codes (also attached as SI) to model a wider variety of situations. Our method models transient reflectance signals using transfer matrix[3] in combination with diffusion simulation.[2] The modelled perovskite film was split into multiple layers, each one with Δn and Δk proportional to the carrier concentration as exemplified in Figure S1. Transfer matrix (TM) then calculates the change in reflectance and thin-film interference based on the carrier distribution in the perovskite film. Our model not only accounts for the two interfaces, the air-film and film-substrate, but also for any interference that originates from the gradient in the refractive index inside the film itself due to inhomogeneous charge carrier

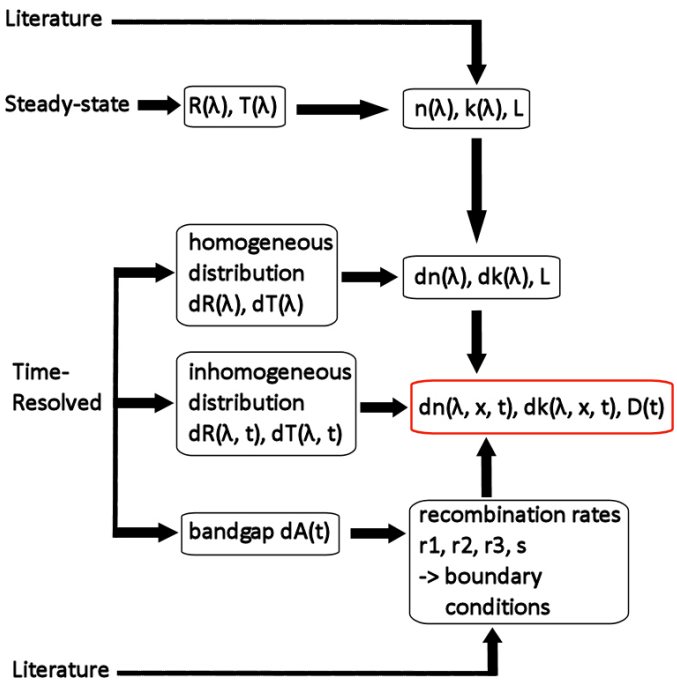

Figure S2: Workflow of the diffusion fit. The TFI model requires three preliminary datasets for the diffusion modelling: 1) an estimate of the complex refractive index (n and k) and the thickness (L) of the film from steady-state measurements and other sources, 2) the photoinduced Δn and Δk acquired from a transient reflectance and transmittance measurement with a uniform or otherwise well-known carrier distribution, and 3) the recombination rates and boundary conditions, which for instance can be acquired from transient absorption measurements of the bandgap. Once these factors are clear, the diffusion can be modelled from a transient reflectance and transmittance measurement with a sufficiently short pump wavelength that generates most of the carriers at the sample surface.

distribution. For the perovskite samples the film was split into 1 nm thick slices whereas the GaAs was split into 3 nm slices.

The workflow chart of the TFI model is presented in Figure S2. The first step in using the TFI model is to estimate the complex refractive index of the material ($\tilde{n} = n + ik$) and thickness of the film. Loper et al.[4] studied the complex refractive index of $MAPbI_3$, which we then modified to match our FAMACs perovskite steady-state spectra as they have very similar optical properties. The absorption at the pump wavelength was acquired from the steady-state measurements for the perovskite samples: while absorption at 500 nm and above could be measured directly from the 500 nm thick samples, the absorbance at 400 nm

is roughly 6, or not measurable directly, therefore thinner 50 nm perovskite films were used in this range to approximate $\tilde{n}$ which was then used to study 500 nm thick films. The GaAs refractive index was taken from the publications of Aspnes et al.[5] and Adachi.[6] There was significant variation in the reported literature values for the GaAs absorption at 825 nm, so we settled on A = 6 for a 9 µu thick layer, which matches $k = 0.1$. The incident angle was approximately 10 degrees for all the reflection measurements.

The Δn and Δk fit was done by using the linear approximation, as presented previously.[1] In short, we modelled how much a very small change in n changes the reflectance and transmittance, and the same for k, and then calculated the Δn and Δk based on experimental ΔR and ΔT by assuming a uniform carrier concentration at a very long (1-5 ns) delay time. In order to ensure the uniform carrier distribution, 600 nm excitation was used for the visible range $\Delta n/\Delta k$ fit and 700 nm excitation for the NIR. The same $\Delta n/\Delta k$ was then used for all other samples, but the thickness and roughness varied from sample to sample. The GaAs film was modelled and fitted the same way as the perovskites except that the 500 nm GaAs film was coated by 20 nm of GaInP from both sides, which were included in the simulation but assumed to have no photoinduced change in the refractive index. The wafer had no coating.

The recombination rate constants (r_1, r_2 and r_3 with units s^{-1}, $cm^3\ s^{-1}$ and $cm^6\ s^{-1}$, respectively) were estimated based on the TAS of the bandgap, as explained in the main text. Figure S3 shows the effect of 2nd and 3rd order recombination: The higher pump power increases the 2nd and 3rd order recombination rates, which hastens the formation of a uniform carrier distribution while the diffusion itself is mostly unaffected. The effects of higher pump power on the TA spectra bandgap bleaching with excitation wavelength of 400 nm are also showcased in Figure S4.

Once we had established the recombination rates and Δn and Δk, and estimated the thickness and roughness of the film based on the interference pattern, the diffusion constant was the only remaining fitting parameter. The exact diffusion fitting settings for each mea-

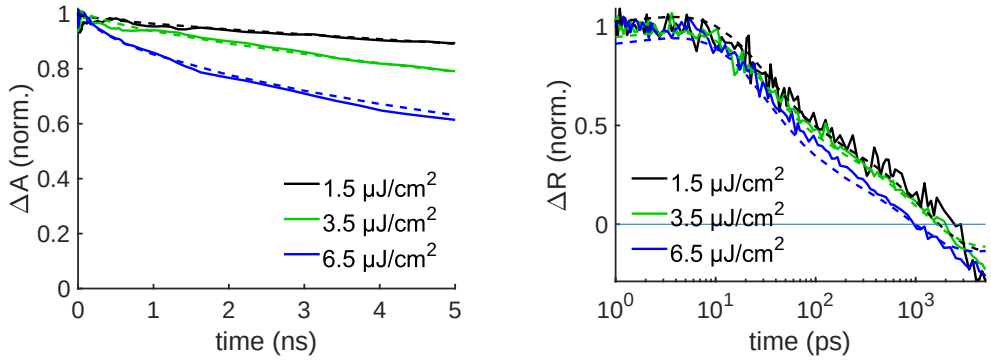

(a) (b)

Figure S3: Diffusion dependence on pump power with 510 nm excitation: (a) Normalized TA signal of the bandgap bleaching with varying pump power (solid lines) compared to the simulated carrier recombination (dashed lines) showing the impact of 2nd and 3rd order recombination. (b) Normalized TR measurements (solid lines) and the modelled signal (dashed lines) with varying pump power at 1159 nm wavelength. The exact simulation settings are given in Table S1 sample 3.

surement are found in Table 1. Depending on the sample the fitting required some roughness (roughness thickness, r.t.) on the perovskite surface, which was modelled as nanopyramids, meaning that there was a gradual shift in refractive index between the bulk perovskite film (bulk thickness, b.t.) and the air. The effect of roughness on the TR signal has been addressed in more detail in one of our previous publications.[2] The average thickness of the film is b.t. plus one third of r.t., which varied from 460 nm to 510 nm depending on the sample and the measurement spot. Both the GaAs wafer and the thin-film were assumed to be smooth (no roughness). Here we also show the maximum bandgap bleaching (b.g.b.) for the perovskite samples, which is assumed to correlate with the pump energies given in the Table 2 of the main text. The absorbance at the excitation wavelength, A, gives the initial carrier distribution.

In the main text we also used the surface carrier concentration (SCC) model to estimate diffusion, which required picking specific measurement wavelengths where the SCC matched with out TM-based model. Figure S5 shows that in many cases the SCC model simply couldn't meaningfully reproduce the TR results: At 550 nm wavelength, where the perovskite

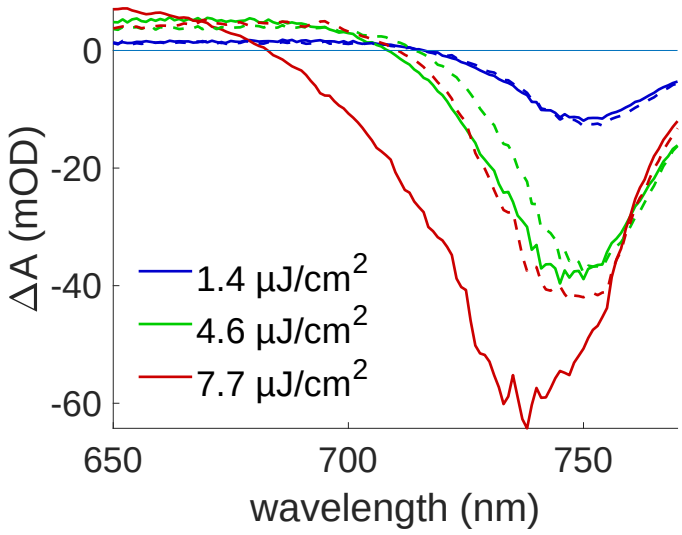

Figure S4: TA response of a perovskite film as a function of pump energy with 400 nm excitation. Solid lines represent the signal at 1 ps and the dashed lines at 1 ns delay time.

Table S1: Diffusion fitting settings

s	ex (nm)	b.g.b.	D_0	D_1	τ	b.t.	r.t.	A	r_1 (10^7)	r_2 (10^{-11})	r_3 (10^{-29})
P1	400	13	0.20	1.20	40	461.5	110	6	3	8	4
		44	0.20	1.20	40	463	110	6	3	8	4
P2	400	74	0.20	1.40	40	437	70	5.5	3	8	4
P3	510	18	0.20	1.30	60	499	30	3.06	0	8	4
		40	0.20	1.30	60	499	30	3.06	0	8	4
		76	0.20	1.40	80	497	30	3.06	0	8	4
P4	600	17	0.20	1.40	80	450	90	1.28	3	8	4
		35	0.20	1.40	80	442.5	110	1.28	5	10	4
		80	0.20	1.40	80	438.1	120	1.28	7	10	4
P5	700	33	0.20	1.60	80	477.5	30	0.72	3	8	4
		66	0.20	1.60	80	483	30	0.72	3	8	4
		113	0.20	1.60	80	476	30	0.72	3	8	8
P6	400–730	27	0.20	1.20	60	457.5	100	6–0.62	3	8	4
GaAs	825	–	120	0	0	9000	0	6	0	72	0.1

film is practically opaque, the TR signal is negative after hot-carrier cooling and then switches to positive, increasing in signal strength up to 10 ps. Our TM-model was able to reasonably reproduce this data because it accounts for the interference effects stemming from the carrier distribution near the surface, whereas the SCC cannot model a situation where the signal changes its sign. At 477 nm both the Δn and Δk are negative (Figure S6(a)) and the SCC and TFI models are a a good match, but at 550 nm the Δn and Δk are close to each other

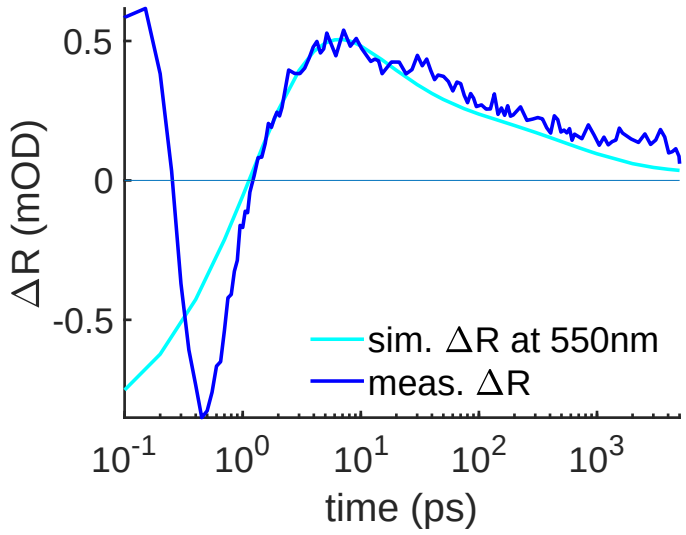

Figure S5: TR data compared to TFI-based simulation with $D = (0.20 + 1.40 \cdot e^{-t/40\,\mathrm{ps}})\,\mathrm{cm}^2\,\mathrm{s}^{-1}$ at 550 nm wavelength. Due to the $\Delta n/\Delta k$ ratio at this specific wavelength, the surface carrier approximation is clearly unable to explain the signal behaviour (it cannot model signals that flip from negative to positive or that increase in strength instead of decreasing) whereas our thin-film interference model gives a reasonable fit.

in strength but opposite in sign, which causes this strange behaviour of the TR signal. In NIR the $\Delta n \gg \Delta k$ (Figure S6(b)), as we have reported previously.[1]

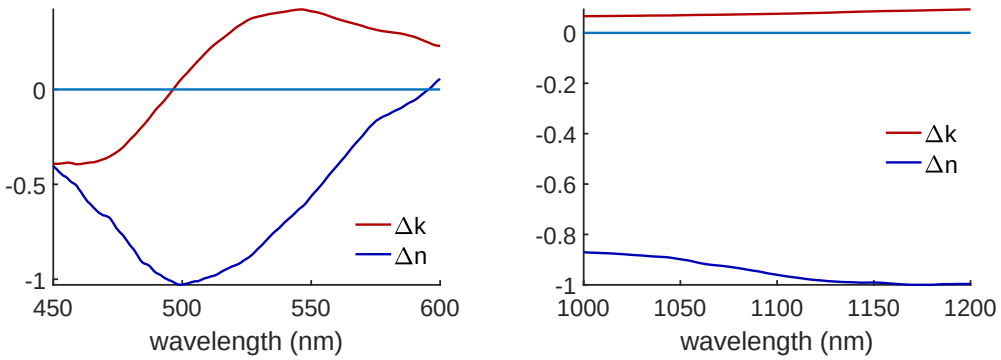

(a) (b)

Figure S6: Normalized Δn and Δk at a) 450-600 nm and b) 1000-1200 nm wavelengths for the perovskite films.

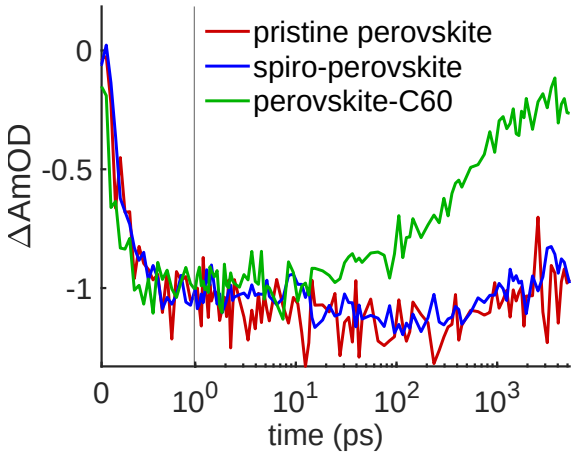

Figure S7: Semilogarithmic normalized bandgap bleaching of a 70 nm thin perovskite film measured at 750 nm wavelength with either C_{60} or spiro-OMeTAD: C_{60} reduces the lifetime whereas spiro-OMeTAD does not, indicating that photoexcited holes do not impact the TA or TR signals. The excitation energy was 2.3 µJ cm^{-2}.

70 nm thin perovskite film measurements and results

Figure S7 shows the lifetime of the bandgap bleaching of a thin pristine perovskite film (70 nm) compared to perovskite with C_{60} or spiro-OMeTAD. The lifetime of a pristine perovskite sample matched that of perovskite-spiro, meaning that hole transfer does not alter the transient signal. In perovskite films as thin as 70 nm the hole and electron transfers should occur fast, and this is the case for perovskite-C_{60}, leading us to conclude that the transient features originate from the photoexcited electron but not the hole. Figure S8 shows the shape of the (a) transient absorption and (b) transient reflectance spectra of the pristine 70 nm perovskite film in the visible range. The pump power was much lower in Figure S7 than in Figure S8, which is why the lifetime is much shorter in the latter. High pump power was necessary to evaluate the 430–600 nm signal.

As portrayed in Figures S8 and S6(a), FAMACs perovskite has a negative transient absorption peak ($\Delta k < 0$) at 460 nm. Because the Δk is negative below 500 nm and positive above 500 nm, the Δn reaches a local minimum at 500 nm, as suggested by Kramers-Kronig relations.

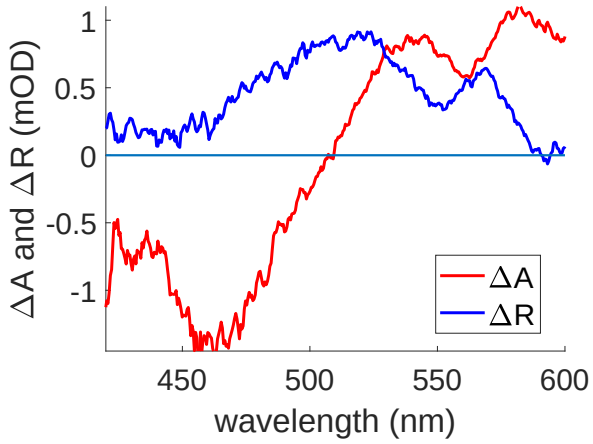

Figure S8: 70 nm thick pristine perovskite film TA and TR spectra at 430 to 600 nm probe wavelengths.

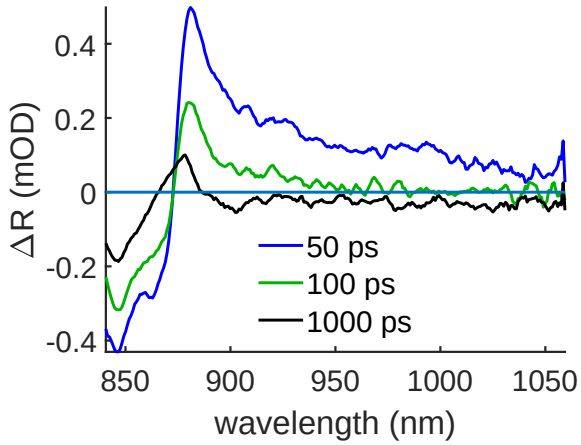

Figure S9: NIR TR spectra of the GaAs wafer with 500 nm excitation. The signal drops to negative at most wavelengths after 100 ps. Earlier delay times of this measurement were shown in the main text Figure 5(b).

Additional GaAs transient data

Figure S9 shows the full TR spectra of the GaAs wafer after 825 nm excitation, matching the Figure 6(b) of the main text. The NIR signal drops almost entirely to negative after 100 ps, but before that it follows the expected behaviour based on the Kramers-Kronig relations.

Figure S9(a-d) shows the full TT and TR spectra of the GaAs thin-film sample from visible range to NIR expect the bandgap region from 760 to 890 nm. The visible range had a negative TA peak at 690 nm with the same lifetime as the NIR signals and another peak at 750 nm which disappeared as the carriers relaxed to the lowest conduction band. The NIR signal on the other hand was dominated by the refractive index change and the thin-film interference with only minimal contribution from the change in absorption (Δk), as can be seen from Figure S11.

Figure S12 is the matching TR spectra to the transient transmittance data of Figure 2(a) of the main text. The TR spectra is quite complex due to thin-film interference and sharp changes in Δn and Δk at the bandgap.

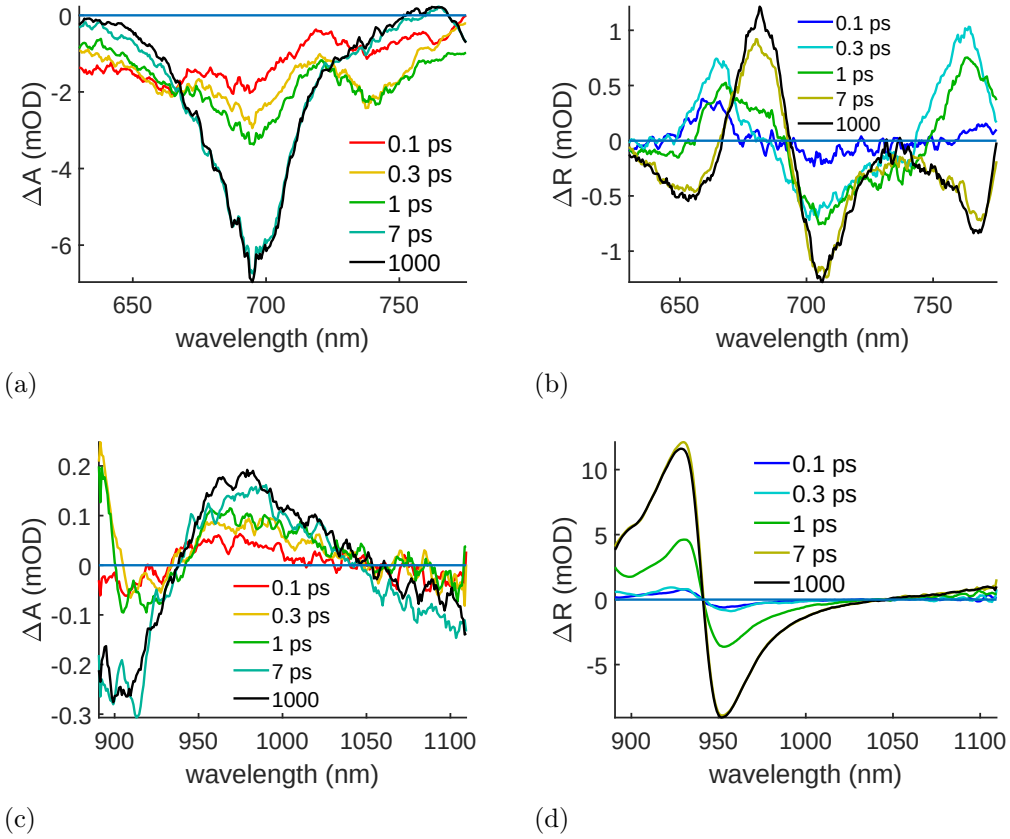

Figure S10: Transient spectra of the GaAs thin film with 600 nm excitation and $2 \cdot 10^{18}\,\mathrm{cm}^{-3}$ carrier density: (a) visible range TA, (b) visible range TR, (c) NIR TA and (d) NIR TR.

Experimental details

Transient absorption and reflectance spectroscopy equipment

The samples were excited by laser pulses generated by Libra F, Coherent Inc., coupled with Topas C, Light Conversion Ltd. A white continuum generator (sapphire crystal for NIR and heavy water for visible range) was used to produce the probe beam. The TA and TR responses were measured using an ExciPro TA spectrometer (CDP, Inc.) equipped with a CCD array for the visible spectral range (460–770 nm), and an InGa diode array for the near-infrared wavelengths.

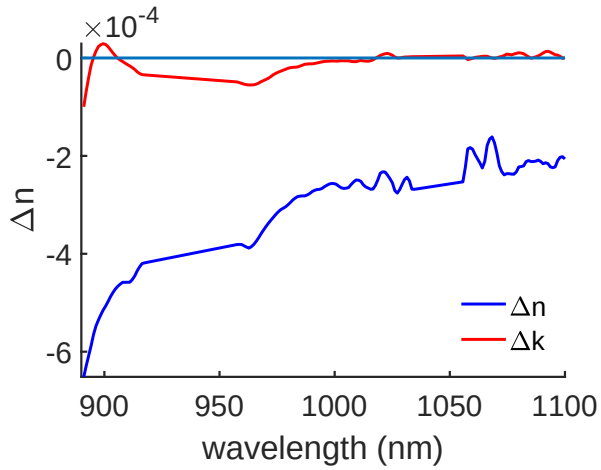

Figure S11: GaAs NIR photoinduced Δn and Δk calculated from Figure S10(c-d) at 1 ns delay time.

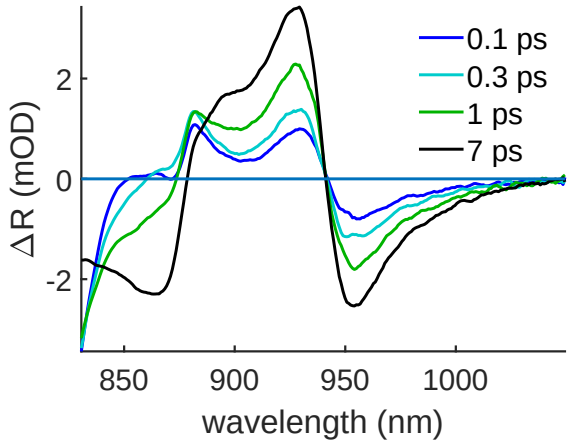

Figure S12: NIR TR of the GaAs thin film with the same pump settings as in the Figure 5(a) of the main text (700 nm excitation).

Perovskite sample preparation

Soda-lime glass (Thermo Scientific^{TM}) or H-K9L glass (UniversityWafer) substrates, 2 cm × 2 cm, were sonicated using an aqueous solution of Hellmanex III solution (2%), acetone and 2-propanol for 15 minutes in each step, successively. The substrates were then treated with UV-ozone for 15 minutes to remove organic residuals and increase hydrophilicity. For the sample with the electron transport layer, C60 ($\tilde{2}$5 nm thickness) was thermally evaporated on the as-cleaned glass substrate. To make a 500 nm thick perovskite film, a concentrated perovskite precursor was prepared containing FAI (0.95 M), PbI_2 (1.1 M), MABr (0.19 M), $PbBr_2$

(0.2 M) and CsI (0.06 M) in anhydrous DMF:DMSO 4:1 (v:v), following a previous report.[7] For a $\tilde{7}$0 nm thick perovskite film, as-prepared concentrated perovskite precursor was further diluted with the anhydrous mixture solvent (DMF:DMSO = 4:1) by a factor of 5. 50 µl perovskite precursor was spin-coated onto either as-cleaned glass substrate (glass/perovskite) or as-formed C60 film (glass/C60/perovskite) at 1000 rpm with 500 rpm/s acceleration for 10 s, directly followed by 6000 rpm with 2500 rpm/s acceleration for 20 s. 5 s prior to the end, 100 µl chlorobenzene were dropped as anti-solving treatment. The perovskite layer was then annealed at 110 °C for 1 h. After annealing, for the sample (glass/perovskite/spiro-OMeTAD) with the hole transport layer, a spiro-OMeTAD layer was spin-coated at 4000 rpm with 2000 rpm/s acceleration for 30 s. The spiro-OMeTAD solution was prepared by adding 36.2 mg spiro-OMeTAD to 1 ml chlorobenzene and 14.4 µl 4-tBP were stirred using a vortex mixer. Then 8.7 µl Li-TFSI solution and 14.5 µl FK209 pre-dissolved in acetonitrile were added to the spiro-OMeTAD solution with concentrations of 520 mg/ml and 300 mg/ml, respectively. C60 was thermally evaporated.

GaAs sample preparation

For the GaAs wafer piece no preparation was performed besides cleaving the 50 mm wafer into quarters for better handling. The wafer info is given in Figure S13. On an identical wafer piece a thin GaAs structure (500 nm GaAs embedded in 20 nm GaInP on both sides) was grown via molecular beam epitaxy in order to isolate it as a membrane. 150 nm of AlAs between the thin film structure and the substrate act as a process layer. A 10 mm × 10 mm chip was cleaved out of the quarter wafer piece. This chip was liquid capillary bonded[8] with the epitaxy side down to a 20 mm × 20 mm glass substrate. The edges of the bonded chip were sealed with glue to ensure the bonding to maintain during all wet-chemical process steps. The sample was mechanically thinned to a thickness of about 100 µm. Additional glue was used to protect a frame of the thinned GaAs substrate with a width of about 1 mm on all edges surrounding the chip. An Ammonia : H_2O_2 solution (1 : 3) was used to remove

the substrate in the center area of the bonded chip. A short dip in buffered HF solution was applied to remove the AlAs layer and other residuals on the thin film's surface.

Parameter	Customer's Requirements	Guaranteed / Actual Values	UOM
ConductType:	S-I	S-I	
Dopant:	GaAs-Undoped	GaAs-Undoped	
Diameter:	50.8±0.4	50.8±0.4	mm
Orientation:	(100) ±0.5°	(100) ±0.5°	
Orientation Angle:	N/A	N/A	
Primary Flat:	EJ (0-1-1)±0.5°	EJ (0-1-1)±0.5°	
PFlat Length:	17±2	17±2	mm
Secondary Flat:	EJ (0-11)±0.5°	EJ (0-11)±0.5°	
SFlat Length:	7±1	7±1	mm
CC:	Min: N/A Max:	Min: N/A Max:	/c.c.
Resistivity:	Min: 1.01E7 Max:	Min: 2.86E8 Max: 2.17E8	ohm.cm
Mobility:	Min: N/A Max:	Min: 3910 Max: 4500	$cm^2/v.s.$
EPD:	Ave <: 5000 Max <:	Ave <: 5000 Max <:	$/cm^2$
Laser Marking:	NONE	NONE	
Thickness:	Min: 325 Max: 375	Min: 325 Max: 375	µm
TTV:	Max: 9.99	Max: 9.99	µm
TIR:	Max: 9.99	Max: 9.99	µm
Bow:	Max: N/A	Max: N/A	µm
Warp:	Max: 9.99	Max: 9.99	µm
Surface:	Side 1: Polished Side 2: Etched	Side 1: Polished Side 2: Etched	
Particle Count:	N/A	N/A	

Quantity:	100	pcs
Area:	300	$Inch^2$
Ingot Number:	0000567142	
Wafer Number:	3-16, 18-29, 31-32, 35-49, 51-71, 73-97, 99-100, 102-109, 111	
Epi-Ready:	Guaranteed for a period of 6 months	

Figure S13: GaAs wafer info.

References

(1) Pasanen, H. P.; Vivo, P.; Canil, L.; Abate, A.; Tkachenko, N. Refractive Index Change Dominates the Transient Absorption Response of Metal Halide Perovskite Thin Films in the near Infrared. *Phys. Chem. Chem. Phys.* **2019**, *21*, 14663–14670.

(2) Pasanen, H. P.; Vivo, P.; Canil, L.; Hempel, H.; Unold, T.; Abate, A.; Tkachenko, N. V. Monitoring Charge Carrier Diffusion across a Perovskite Film with Transient Absorption Spectroscopy. *J. Phys. Chem. Lett.* **2020**, *11*, 445–450.

(3) Yariv, A.; Yeh, P. *Photonics: Optical Electronics in Modern Communications*, 6th ed.; Oxford University Press, 2007.

(4) Löper, P.; Stuckelberger, M.; Niesen, B.; Werner, J.; Filipič, M.; Moon, S.-J.; Yum, J.-H.; Topič, M.; De Wolf, S.; Ballif, C. Complex Refractive Index Spectra of $CH_3NH_3PbI_3$ Perovskite Thin Films Determined by Spectroscopic Ellipsometry and Spectrophotometry. *J. Phys. Chem. Lett.* **2015**, *6*, 66–71.

(5) D. E. Aspnes, R. A. L., S. M. Kelso; Bhat, R. Optical properties of $Al_xGa_{1-x}As$. *J. Appl. Phys.* **1986**, *60*, 754–767.

(6) Adachi, S. Optical dispersion relations for GaP, GaAs, GaSb, InP, InAs, InSb, $Al_xGa_{1-x}As$, and $In_{1-x}Ga_xAs_yP_{1-y}$. *J. Appl. Phys.* **1989**, *66*, 6030–6040.

(7) Zhang, H.; Liu, M.; Yang, W.; Judin, L.; Hukka, T. I.; Priimagi, A.; Deng, Z.; Vivo, P. Thionation Enhances the Performance of Polymeric Dopant-Free Hole-Transporting Materials for Perovskite Solar Cells. *Adv. Mater. Interfaces* **2019**, *6*, 1–10.

(8) Yablonovitch, E.; Hwang, D. M.; Gmitter, T. J.; Florez, L. T.; Harbison, J. P. Van der Waals bonding of GaAs epitaxial liftoff films onto arbitrary substrates. *Applied Physics Letters* **1990**, *56*, 2419–2421.